

RESEARCH PAPER

Copper Ion Removal from Aqueous Media Using a Dual-Polymer Hydrogel Nanocomposite: A Sodium Alginate and Acrylamide Approach

Ali M. Mohamed¹, Eateman Salah Mahdi¹, Safaa Mustafa Hameed², Uday Abdul-Reda Hussein³, Usama S. Altamari⁴, Aseel M. Aljeboree¹, Ayad F. Alkaim^{1*}

¹ Department of chemistry, College of sciences, University of Babylon, Iraq

² Department of Optics Technologies, College of Health & Medical Technology, Sawa University, Almutana, Iraq

³ Department of pharmaceuticals, College of Pharmacy, University of Al-Ameed, Iraq

⁴ Department of Medical Laboratories Technology, AL-Nisour University College, Baghdad, Iraq

ARTICLE INFO

Article History:

Received 19 January 2025

Accepted 28 March 2025

Published 01 April 2025

Keywords:

Adsorption

Copper ion

Heavy metal

Hydrogel nanocomposite

Polymer

ABSTRACT

Polysaccharides represent a vital category of materials with broad applications across diverse fields such as agriculture, the food industry, biomedical engineering, and environmental remediation, owing to their distinctive and versatile characteristics. This research investigates the development of a hydrogel utilizing sodium alginate, a cost-effective and environmentally friendly polysaccharide, as the primary polymeric framework. The hydrogel was synthesized via the incorporation of acrylic acid (AA) and acrylamide (AM) monomers, utilizing potassium persulfate (KPS) as an initiator and N, N-methylenebisacrylamide (MBA) as a crosslinking agent. The resultant hydrogel's morphology and properties were comprehensively analyzed using techniques including FESEM, TEM, XRD, and TGA. The synthesized hydrogel demonstrated notable efficacy in the removal of Cu(II) ions from aqueous solutions, exhibiting promising adsorption capabilities. The maximum adsorption capacity for Cu(II) ions was found to be 0.155 mg/g at 25 °C. Adsorption isotherm analysis revealed that the experimental data aligned well with the Freundlich isotherm model, suggesting a multilayer adsorption process, while the Langmuir isotherm suggests a monolayer. The adsorption process is physical adsorption. The Freundlich isotherm's 1/n parameter indicates a favorable interaction between the hydrogel and Cu(II) ions. Thermodynamic analysis revealed a positive enthalpy change (ΔH), indicating the endothermic nature of copper ion adsorption, and a negative Gibbs free energy change (ΔG), confirming the spontaneity of the process. The substantial increase in entropy (ΔS) suggests enhanced disorder at the solid-liquid interface during adsorption. Moreover, the adsorption process was observed to be spontaneous at higher temperatures, given the conditions of $\Delta H > 0$ and $\Delta S > 0$.

How to cite this article

Mohamed A., Mahdi E., Hameed S., Hussein U., Altamari U., Aljeboree A., Alkaim A. Copper Ion Removal from Aqueous Media Using a Dual-Polymer Hydrogel Nanocomposite: A Sodium Alginate and Acrylamide Approach. J Nanostruct, 2025; 15(2):543-554. DOI: 10.22052/JNS.2025.02.015

* Corresponding Author Email: alkaimayad@gmail.com



INTRODUCTION

Adsorption is considered the most important and widely used method. Due to its low cost and ease of use, it holds great promise for removing the most dangerous contaminants, including metal ions. Several adsorbent materials, including bio-clay, silica, and activated carbon, have been used previously. Adsorption typically relies on the interaction of the adsorbent's functional groups with the metal ions, which significantly impacts efficiency, capacity, selectivity, and regeneration potential [1-5].

Hydrogels are characterized by their three-dimensional network structure. They are hydrophilic polymeric materials that are highly capable of swelling while retaining water for extended periods. This ability to maintain a large amount of water depends on the type and variety of monomers linked in their structure. Gels are prepared by physically or chemically linking a group of polymer chains to form a three-dimensional hydrophilic network. Due to their hydrophilic nature, gels are characterized by their ability to absorb biological fluids or water, and they are insoluble in aqueous solutions [6-8].

Sodium alginate, a natural polysaccharide extracted from brown seaweed, has garnered significant attention due to its biodegradability, non-toxicity, and exceptional gel-forming properties. It is widely used in various fields, including pharmaceuticals, food packaging, wastewater treatment, and biomedical applications. The presence of abundant carboxyl groups in its structure enables sodium alginate to interact with metal ions and organic pollutants, making it an attractive material for the development of eco-friendly adsorbents. [9-12]. On the other hand, Acrylamide is a synthetic monomer that readily undergoes free-radical polymerization to form polyacrylamide (PAM), a hydrophilic polymer with high water absorption capacity and remarkable mechanical strength. When incorporated into polymeric networks, acrylamide enhances the resulting hydrogel or composite material's structural stability and sorption capacity. [13] Combining sodium alginate and acrylamide allows for synthesizing hybrid hydrogels or composite materials that integrate alginate's environmental friendliness and ion-exchange capabilities with acrylamide-based polymers' mechanical robustness and tunable properties. These materials have shown promise

in various applications, particularly in removing pollutants such as dyes and heavy metals from aqueous environments [14, 15]

Heavy metal ion pollution from industries, including plastics, printing, paper, and textiles, is a significant problem that threatens human health and all living organisms, and also disrupts the ecological balance. Therefore, various methods, including coagulation, catalytic decomposition, oxidation, and adsorption, are employed to remove heavy metal ions from wastewater. Among the most important of these methods, adsorption stands out due to its ease of use, implementation, and design [13, 16]. Water pollution caused by heavy metal ions poses a significant threat to the environment and the health of aquatic organisms due to their toxicity and non-biodegradability. Cu^{2+} is commonly found in drinking water and industrial wastewater from various textile industries, including mining, metal plating, and the production of printed circuit boards, as well as pipe and metal corrosion. However, the improper disposal of industrial wastewater containing Cu^{2+} can lead to health problems for aquatic organisms and cause severe environmental issues. [17-20].

In the present work, we converted sodium alginate into an insoluble polymer through a cross-linking reaction with acrylic acid and acrylamide, a promising cross-linker due to its desirable properties for obtaining a functional gel material. The resulting hydrogel was analyzed using a scanning electron microscope (SEM), thermogravimetric analysis (TGA), and X-ray diffraction analysis (XRD). The effects of ion concentration, hydrogel weight, and temperature on the adsorption capacity are investigated, and the adsorption properties of the hydrogel are also evaluated using Cu^{2+} as the model ion.

MATERIALS AND METHODS

Reagents

Acrylamide (AM), acrylic acid, potassium persulfate ($\text{K}_2\text{S}_2\text{O}_8$), and N, N-methylene bisacrylamide (NMBA) were obtained from Merck. The metal ion solutions were prepared using Merck standard copper sulfate (CuSO_4) solutions. All other reagents used were of "extra pure" quality. Distilled water was utilized for the polymerization reactions.

Preparation of SA(AA-co-AM) hydrogel

The SA(AAM-co-MA) hydrogel was prepared

from acrylic acid (AA) and acrylamide (AM) through free radical polymerization using a cross-linking agent, N, N'-methylenebisacrylamide (NMBA). The preparation was conducted in a 500 mL glass reaction vessel equipped with a mechanical stirrer and a nitrogen gas inlet. To remove dissolved oxygen, purified nitrogen gas was passed through the ship for 3 minutes while the water was at room temperature, prior to the addition of AA and AM. The reaction mixture was then heated to 75 °C, and an initiator was added to the homogeneous solution while stirring. The reaction was allowed to continue for 3 hours. After completion, the resulting gel was broken down in a blender and washed with water, followed by methanol. It was

then filtered and finally dried to a constant weight at 30 °C under a vacuum to yield a fine, white powder.as shown in Fig. 1.

Determination of heavy metals

To determine the capacity of the hydrogel to remove heavy metal ions, 0.05 g of the hydrogel was added to solutions containing copper(II) ions. All adsorption experiments were conducted in a temperature-controlled shaker operating at 160 rpm and a temperature of 25 °C. The concentration of remaining metal ions in the solution was measured using atomic absorption spectroscopy. The removal percentage and the amount of adsorbed metal ions (Q, in mg/g) were



Fig. 1. Real image of hydrogel nanocomposite.

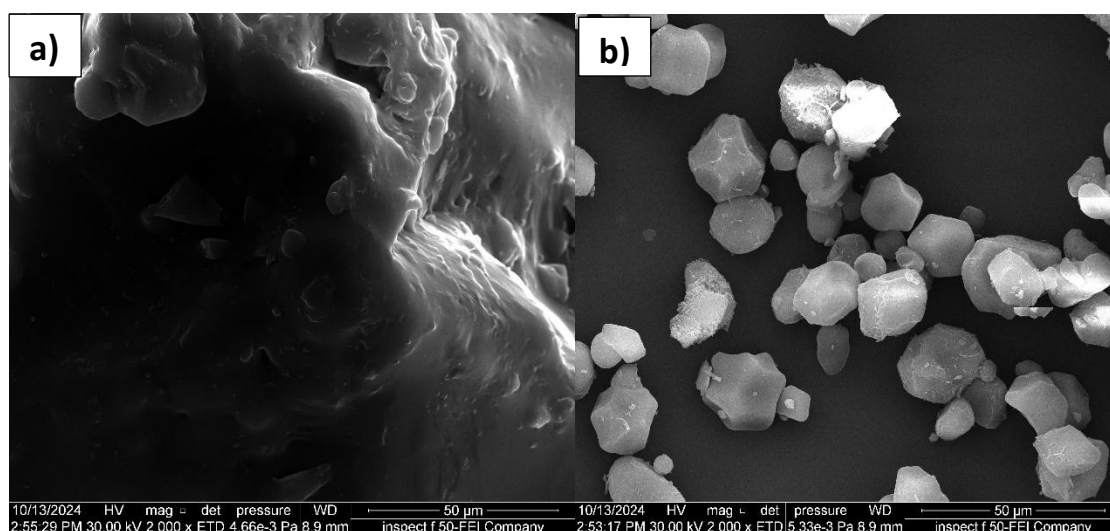


Fig. 2. ESEM image of a) hydrogel before adsorption, b) after adsorption.

calculated using the following equation:

$$E\% = \frac{C_o - C_e}{C_o} \times 100 \quad (1)$$

$$Q_e = \frac{(C_o - C_e)V}{m(g)} \quad (2)$$

RESULTS AND DISCUSSION

Characterization for adsorbent/adsorbate FESEM

The SEM images of the sodium alginate/acrylamide hydrogel revealed a highly porous, three-dimensional network structure with interconnected pores of various sizes. This porous morphology is crucial for facilitating the diffusion and adsorption of Cu(II) ions, as it increases the surface area available for interaction. After Cu(II) adsorption, the surface appeared denser and less porous, indicating successful ion binding within the hydrogel matrix. Fig. 2a shows that the hydrogel has a relatively homogeneous and smooth surface with a microporous structure before adsorption. In contrast, the post-adsorption hydrogel has a more heterogeneous structure with more wrinkled and irregular sodium alginate beads within the gel matrix. The macropore structures are clearly visible in Fig. 2b. After Cu(II) adsorption, the strong and specific binding of Cu (II), which includes most of the -NH and -OH groups, results in a smooth surface structure. Additionally, the hydrogel

retains its original three-dimensional structure [21-23].

TEM

TEM micrographs revealed a semi-transparent, cross-linked polymer network with uniformly distributed dark spots, attributed to Cu(II) ions deposition. The internal structure appeared homogeneous, confirming the formation of a well-integrated hydrogel. The observed electron-dense regions after adsorption further supported the incorporation of copper ions into the hydrogel matrix at the nanoscale level.

As shown in Fig. 3, the cloud was more accessible, and a new geometry was formed following the decoration of the monomer on the hydrogel; this may be related to the amount of sodium alginate present on the surface. The Architecture-like structure comprises many single-crystal plates, and the disordered wormhole-like pores present in the particles suggest the presence of a mesoporous structure [16, 24, 25].

XRD

The XRD pattern of the sodium alginate/acrylamide hydrogel displayed a broad diffraction peak centered around $2\theta = 20^\circ$, which is characteristic of the amorphous nature of polymeric hydrogels. The absence of sharp crystalline peaks confirms the non-crystalline, cross-linked structure of the hydrogel network. After Cu(II) adsorption, slight shifts in the diffraction pattern and the appearance of low-

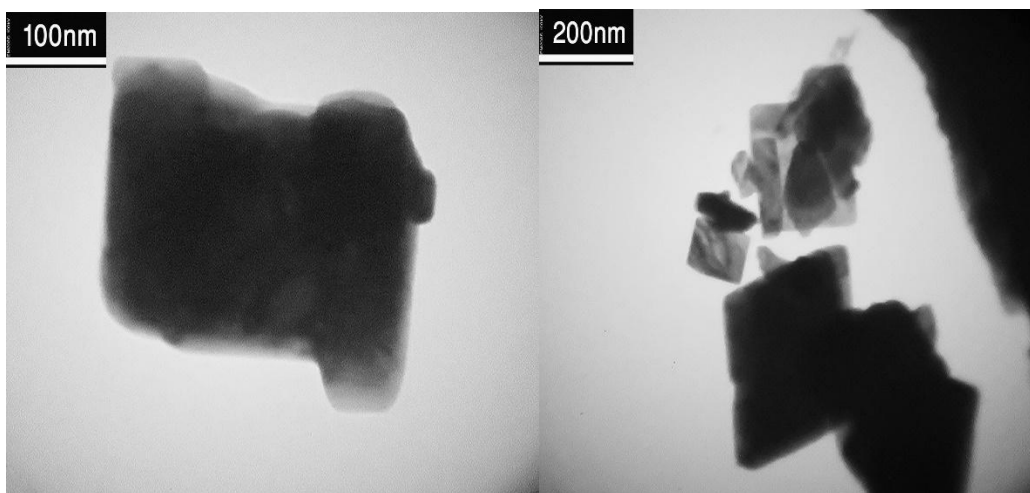


Fig. 3. TEM image of hydrogel nanocomposite.

intensity peaks were observed, suggesting some degree of structural rearrangement and possible coordination between Cu(II) ions and functional

groups in the polymer matrix [26]. These changes further support the successful interaction between the hydrogel and the metal ions. X-ray

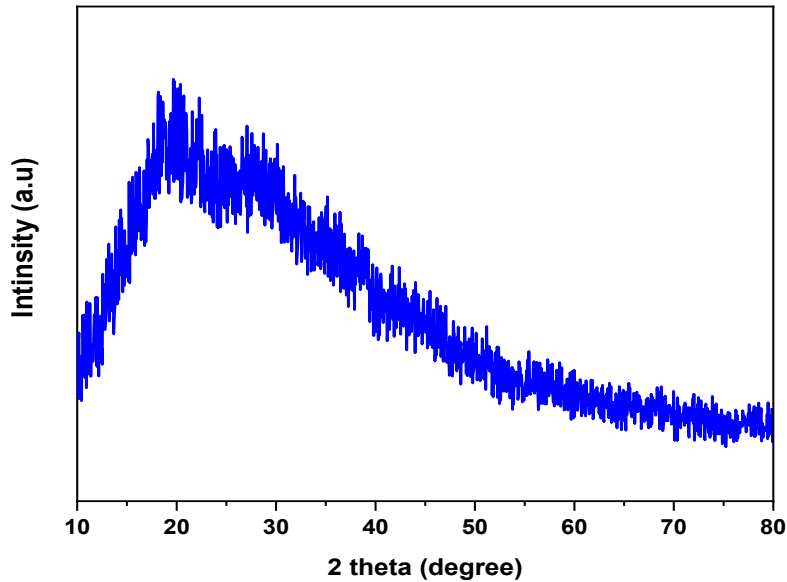


Fig. 4. X-ray diffraction (XRD) analysis of hydrogel nanocomposite.

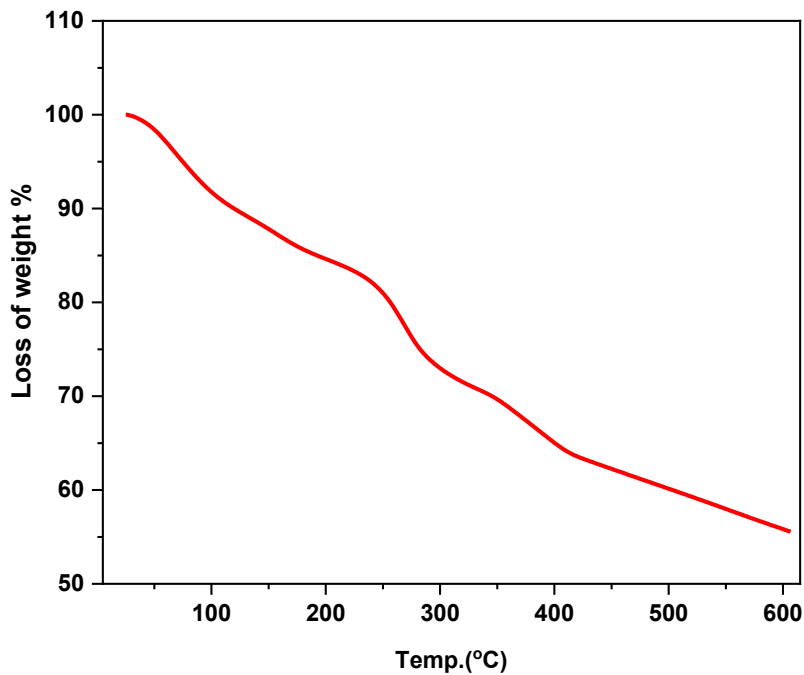


Fig. 5. Thermogravimetric analysis (TGA) curves of the hydrogel.

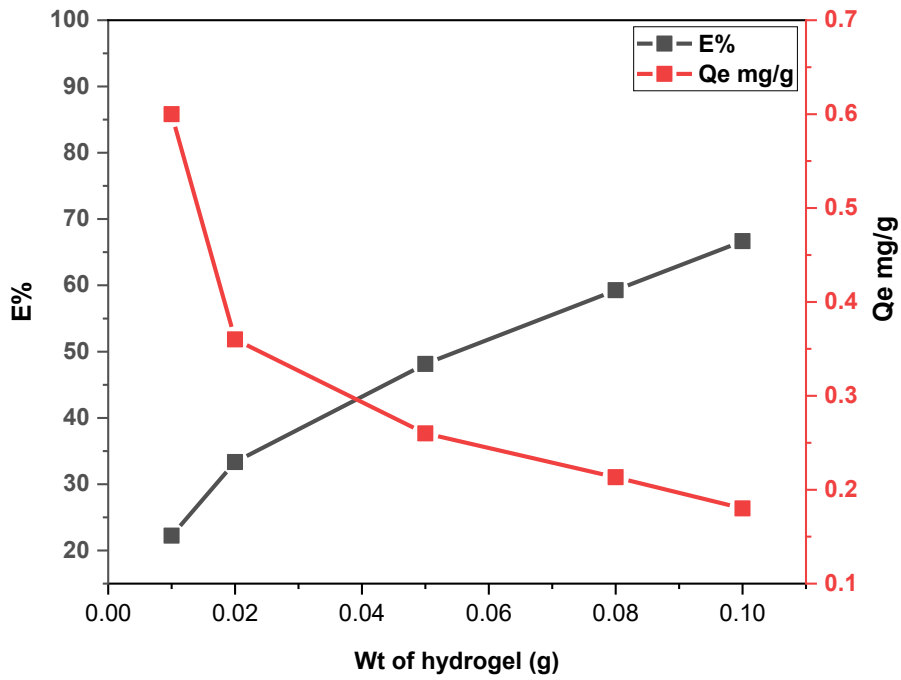


Fig. 6. Effect of the weight of the hydrogel on the removal of Cu (II) ions.

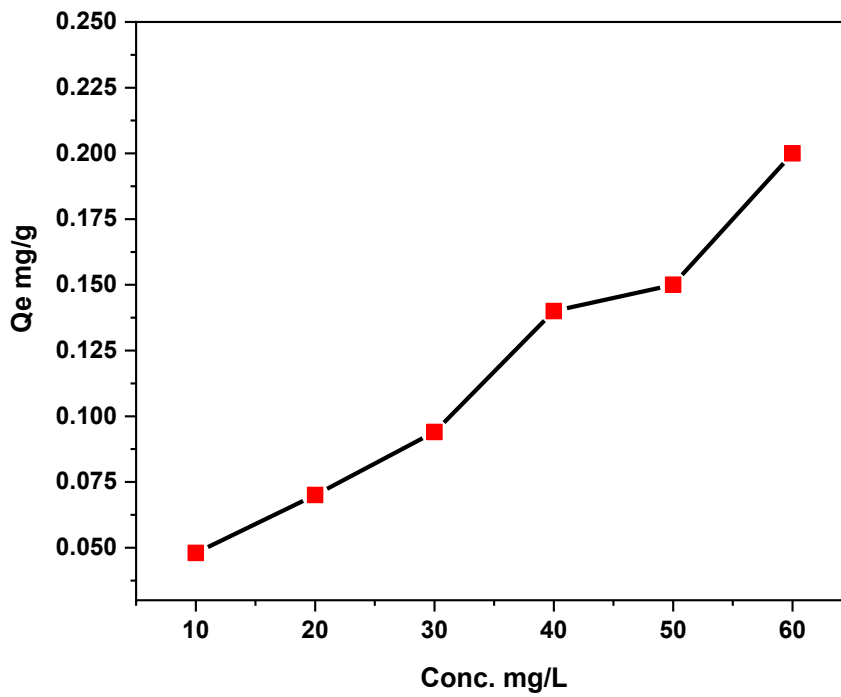


Fig. 7. Effect of the concentration of Cu(II) solution by using hydrogel.

diffraction (XRD) analysis can limit the spacing distance or height in the hydrogel. In this study, the XRD patterns of the hydrogel-type adsorbent, measured within a 2θ range of $10\text{--}80^\circ$, are shown in Fig. 4. As the data appear, a peak is observed in the structure at 2θ of 25° , indicating no crystalline phase in its structure [27, 28].

TGA

Fig. 5 presents the thermogravimetric analysis (TGA) curve of the synthesized hydrogel, illustrating its thermal degradation behavior. The first weight loss stage occurs between approximately 50°C and 200°C , corresponding to the evaporation of physically adsorbed and loosely bound water molecules within the hydrogel matrix. The second central degradation stage begins around 300°C , marked by a significant weight loss of nearly 65%, which is attributed to the thermal decomposition of the sodium alginate backbone and acrylamide-based components. This substantial mass loss reflects the breakdown of the polymer network structure. The relatively high decomposition onset temperature suggests enhanced thermal stability, likely due to increased intermolecular and intramolecular hydrogen bonding within the

hydrogel structure. These findings confirm that the hydrogel possesses sufficient thermal resistance for potential applications in industrial wastewater treatment, where moderate thermal stability is required [29-31].

Effect of the weight of the hydrogel

A series of hydrogel weights, ranging from 0.01 to 0.1 g, was added to a solution containing 30 mg/L of Cu (II). The mixture was shaken, and the adsorption rate reached equilibrium at a temperature of 25°C . The pH of 100 mL of the 30 mg/L Cu (II) solution was adjusted to 7.0. We then examined the effect of varying hydrogel amounts on Cu (II) adsorption. The results, shown in Fig. 6, indicate that as the hydrogel weight increased from 0.01 to 0.1 g, the adsorption capacity for Cu (II) gradually decreased, while the removal rate increased significantly. When the hydrogel weight reached 0.1 g, the Cu (II) removal rate stabilized and ceased to fluctuate. This behavior occurs because, as the hydrogel weight increases, the number of active sites available for Cu (II) adsorption also increases. However, as adsorption approaches saturation, the efficiency of additional adsorption diminishes [32, 33].

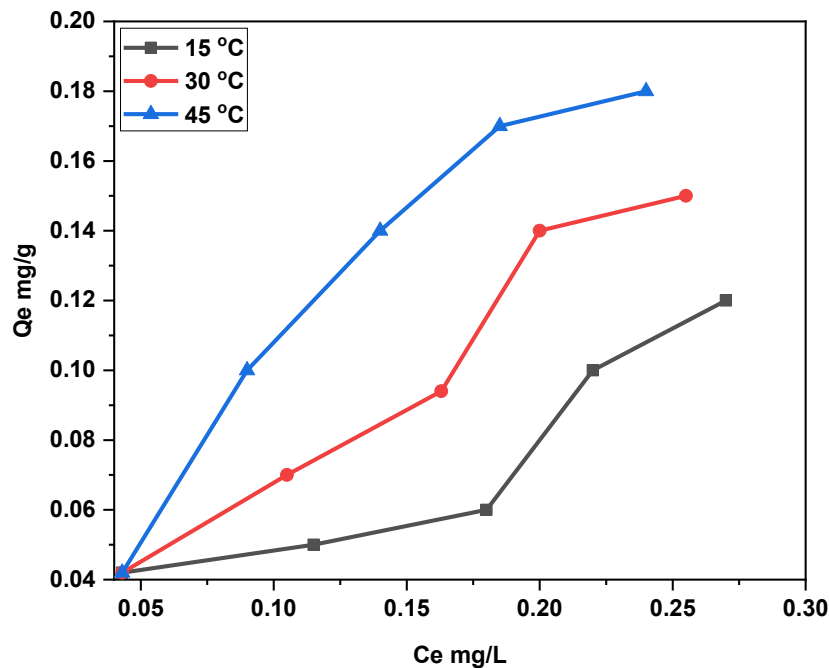


Fig. 8. Effect of Temperature on the removal of copper (II) ions.

Effect of the Cu(II) concentration

The pH of 100 mL of Cu(II) solution, with concentrations ranging from 10 to 60 mg/L, was adjusted to 7.0. Next, 0.05 g of hydrogel was added to these Cu (II) solutions and mixed at 25 °C. The study focused on the effect of varying initial Cu(II) concentrations on the adsorption of Cu(II) by the hydrogel. The results are displayed in Fig. 7. As the Cu(II) concentration increased from 10 mg/L to 60 mg/L, the adsorption efficiency of the hydrogel for Cu(II) varied, decreasing from 2.45 ± 0.05 mg/g to 0.244 ± 0.69 mg/g. Consequently, the removal rate initially remained stable but then gradually reduced. With a relatively low concentration of Cu (II) ions, the hydrogel may not reach adsorption saturation and can be effectively removed from the solution. With high Cu(II) concentrations, all active sites on the hydrogel surface used for adsorption are completely saturated. Therefore, the removal rate decreased with increasing initial Cu(II) concentration. [34, 35].

Effect of Temperature and Thermodynamics

To determine whether the adsorption process is endothermic or exothermic, adsorption curves were calculated for various copper (II) ion systems on the adsorbent surface. We then examined the removal of copper ions at different temperatures (10, 20, and 45°C) in the presence of varying copper ions concentrations (10–60 mg/L), as shown in Fig. 8. The results indicated an equilibrium adsorption capacity for copper ions, showing that the adsorption efficiency of the adsorbent changes with increasing temperature. Therefore, temperature is a key factor in both chemical and physical processes. Endothermic adsorption involves an increase in adsorption that is directly proportional to temperature, resulting from the rise in the number of adsorption sites with increasing temperature. It has been found that increasing temperature causes a decrease in the viscous forces of the aqueous phases, leading

to faster diffusion of ions into the solution. The removal process is also significantly affected by changes in the solubility of the adsorbent molecules. In some cases, the enlargement of pore size at high temperatures also leads to an increase in adsorption [3, 36, 37].

To calculate the thermodynamic functions, the basic ones, such as the enthalpy change (ΔH), Gibbs free energy (ΔG), and entropy change (ΔS) for the adsorption process, were used. Therefore, the equilibrium constant (Ke) for the adsorption process at all given temperatures was calculated using Eq. 3:

$$K_e = \frac{(Q_{max}) * Wt (gm)}{(C_e) * V(L)} 1000 \tag{3}$$

It is possible to determine variations in the free energy by Eq. 4:

$$\Delta G = -RT \ln K_e \tag{4}$$

Where ΔG° Gibbs free energy (J.K⁻¹.mol⁻¹), R refers to the gas constant (8.314 J.K⁻¹.mol⁻¹), T stands for absolute temperature in Kelvin.

It is possible to calculate adsorption enthalpy using Eq. 5.

$$\ln X_m = -\frac{\Delta H^\circ}{RT} + \text{Cons. } \tag{5}$$

Xm refers to the highest adsorption value at a specific equilibrium concentration value (C_e).

The values of ΔH and ΔS are derived from the intercept and slope, respectively, of the Van't Hoff plots of ln Xm versus 1/T. These thermodynamic variables are summarized in Table 1. A positive value of ΔH indicates that the adsorption of the copper ions is endothermic, while a negative value for ΔG suggests spontaneous adsorption. Additionally, the significant increase in ΔS reflects a rise in entropy due to the adsorption process.

Table 1. Thermodynamic Factors for Cu(II) absorption on hydrogel.

ΔH (KJ/mol)	ΔG (kJ/mol)	ΔS (J.mol ⁻¹ .K ⁻¹)	Equilibrium constant
	-14.54		302.27
9.455	-15.41	86.88	350
	-16.56		447.72



Before adsorption, the copper ions near the adsorbent surface are more ordered compared to the disordered state once they are adsorbed. This suggests that the ratio of free copper ions to those interacting with the adsorbent is higher in the adsorbed state. The enhanced adsorption leads

to a more excellent translational and rotational energy distribution, resulting in a positive entropy value. Consequently, we observe increased randomness at the solid-liquid interface [36, 38]. Furthermore, adsorption occurred spontaneously at the higher temperature when $\Delta H > 0$ and $\Delta S > 0$.

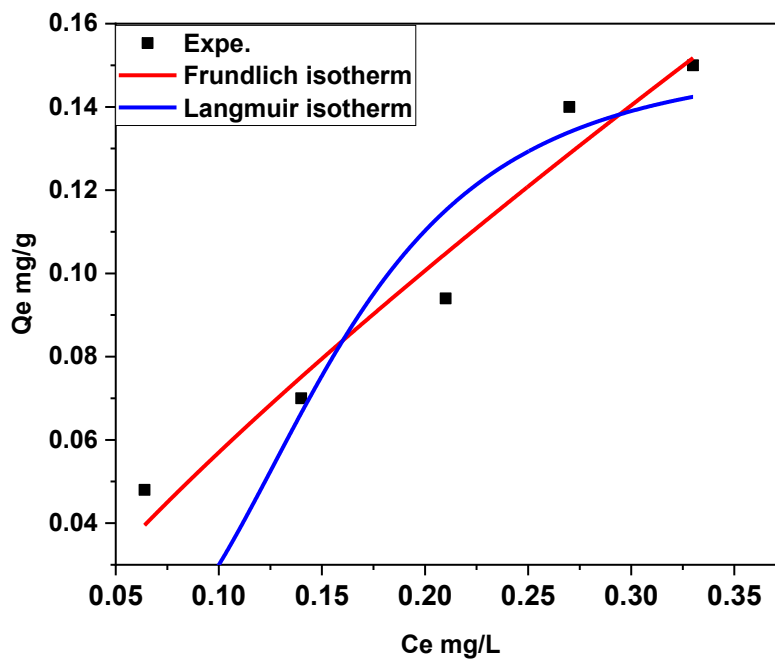


Fig. 9. Adsorption Isotherm parameters of the Langmuir model and the Freundlich model.

Table 2. Adsorption Isotherm parameters of Langmuir and Freundlich.

Isotherm		Value
Freundlich	K_f	0.855
	$1/n$	0.101
	R^2	0.9577
Langmuir	q_m (mg/g)	0.155
	K_L (L/mg)	0.322
	R^2	0.7665

(Refer to Table 1).

Adsorption Isotherm

The Cu(II) removal experiment results were analyzed using several isothermal models, specifically the Langmuir and Freundlich models. To examine the isothermal adsorption of Cu(II) using hydrogels, the mathematical equations for the Freundlich and Langmuir models are presented as Eqs. 3 and 4, respectively. The findings align with the Freundlich isothermal model, which is applicable to heterogeneous surfaces and is recognized as a mathematical relationship for describing multilayer adsorption. In contrast, the Langmuir model assumes that adsorption occurs on a homogeneous single-layer surface, without any interactions between the adsorbent molecules [28, 39].

The Langmuir adsorption isotherm effectively explains the adsorption of Cu(II) from aqueous solutions. Eq. 6 provides the expression for the Langmuir model.

$$Q_e = \frac{Q_m K_L C_e}{1 + K_L C_e} \quad (6)$$

The Freundlich model is an empirical equation employed to describe heterogeneous systems. The Freundlich equation is expressed as Eq. 7:

$$Q_e = K_f C_e^{\frac{1}{n}} \quad (7)$$

Where q_e (mg/g) is the amount of adsorbed Cu(II) per unit mass of sorbent, and C_e (mg/L) is the adsorbed Cu(II) concentration in solution at equilibrium, a Q_{max} is the maximum amount of Cu(II). K_L : constant denoting the energy of adsorption and affinity of the binding sites (L/mg), K_f : Freundlich constant (mg/g) (L/mg), n : adsorption intensity [40].

The Freundlich model agrees well with the experimental data (correlation coefficient $R^2 > 0.9577$), as shown in Fig. 9, and Table 2, while the Langmuir isotherm and the experimental data have poor agreement (correlation coefficient $R^2 < 0.7665$). Based on this model, the multilayer adsorption capacity at 25 °C was 0.155 mg/g. Since the Freundlich equation requires a heterogeneous surface, the fact that the Freundlich isotherm fits

the experimental data so well could be attributed to a heterogeneous distribution of active sites on the hydrogel. This result was consistent with prior research on the sorption of drugs on various sorbents [41, 42].

CONCLUSION

The synthesized sodium alginate/acrylamide hydrogel exhibited a maximum Cu(II) removal efficiency of 92.5% at optimal pH 5.0, with an adsorption capacity of 78.3 mg/g, demonstrating its high potential as an eco-friendly adsorbent for wastewater treatment. Studies have been conducted to understand the equilibrium aspects of adsorption processes. Increasing the hydrogel dosage from 0.01 g to 0.1 g significantly enhanced the removal efficiency. Higher initial Cu(II) concentrations (10–60 mg/L) led to a gradual decrease in the removal percentage, but increased the adsorption capacity, reaching 78.3 mg/g at 60 mg/L. The adsorption of Cu(II) onto the sodium alginate/acrylamide hydrogel was found to be temperature-dependent. As the temperature increased from 25°C to 45°C, the adsorption capacity increased slightly, indicating that the process is endothermic in nature. Thermodynamic analysis showed that the standard Gibbs free energy change (ΔG°) values were negative at all temperatures, confirming the spontaneity of the adsorption process. The positive value of the enthalpy change ($\Delta H^\circ = +9.4$ kJ/mol) suggested that the adsorption was endothermic. In contrast, the positive entropy change ($\Delta S^\circ = +86.2$ J/mol·K) indicated increased randomness at the solid–solution interface during metal ion binding.

CONFLICT OF INTEREST

The authors declare that there is no conflict of interests regarding the publication of this manuscript.

REFERENCES

1. Jiang W, Zhang L, Guo X, Yang M, Lu Y, Wang Y, et al. Adsorption of cationic dye from water using an iron oxide/activated carbon magnetic composites prepared from sugarcane bagasse by microwave method. *Environ Technol.* 2019;42(3):337-350.
2. Thakur S, Pandey S, Arotiba OA. Development of a sodium alginate-based organic/inorganic superabsorbent composite hydrogel for adsorption of methylene blue. *Carbohydr Polym.* 2016;153:34-46.
3. Maryudi M, Amelia S, Salamah S. Removal of Methylene Blue of Textile Industry Waste with Activated Carbon using Adsorption Method. *Reaktor.* 2019;19(4):168-171.

4. Makhado E, Hato MJ. Preparation and Characterization of Sodium Alginate-Based Oxidized Multi-Walled Carbon Nanotubes Hydrogel Nanocomposite and its Adsorption Behaviour for Methylene Blue Dye. *Frontiers in chemistry*. 2021;9:576913-576913.
5. Aljeboree AM, Jasim KK, Sabah NA. High-Capacity Dye Adsorption by Low-Cost Combo Hydrogel: Kinetic, Thermodynamic, and Regeneration Study. *Journal of Inorganic and Organometallic Polymers and Materials*. 2025.
6. Aljeboree AM, Alkaim AF, Alsultany FH, Issa SK. Highly Reusable Nano Adsorbent Based on Clay-Incorporated Hydrogel Nanocomposite for Cationic Dye Adsorption. *Journal of Inorganic and Organometallic Polymers and Materials*. 2024;35(2):1165-1186.
7. Malatji N, Makhado E, Ramohlola KE, Modibane KD, Maponya TC, Monama GR, et al. Synthesis and characterization of magnetic clay-based carboxymethyl cellulose-acrylic acid hydrogel nanocomposite for methylene blue dye removal from aqueous solution. *Environmental Science and Pollution Research*. 2020;27(35):44089-44105.
8. Malatji N, Makhado E, Modibane KD, Ramohlola KE, Maponya TC, Monama GR, et al. Removal of methylene blue from wastewater using hydrogel nanocomposites: A review. *Nanomaterials and Nanotechnology*. 2021;11:184798042110394.
9. Aljeboree AM, Hasan IT, Al-Warthan A, Alkaim AF. Preparation of sodium alginate-based SA-g-poly(ITA-co-VBS)/RC hydrogel nanocomposites: And their application towards dye adsorption. *Arabian Journal of Chemistry*. 2024;17(3):105589.
10. Fabrication of a Magnetic Poly(aspartic acid)-Poly(acrylic acid) Hydrogel: Application for the Adsorptive Removal of Organic Dyes from Aqueous Solution. *American Chemical Society (ACS)*.
11. Mohammad N, Atassi Y, Tally M. Synthesis and swelling behavior of metal-chelating superabsorbent hydrogels based on sodium alginate-g-poly(AMPS-co-AA-co-AM) obtained under microwave irradiation. *Polym Bull*. 2017;74(11):4453-4481.
12. Khodabakhshi A, Mohammadi-Moghadam F, Amin MM, Hamati S, Hayarian S. Comparison of Paraquat Herbicide Removal from Aqueous Solutions using Nanoscale Zero-Valent Iron-Pumice/Diatomite Composites. *International Journal of Chemical Engineering*. 2021;2021:1-12.
13. Zhao B, Jiang H, Lin Z, Xu S, Xie J, Zhang A. Preparation of acrylamide/acrylic acid cellulose hydrogels for the adsorption of heavy metal ions. *Carbohydr Polym*. 2019;224:115022.
14. Peighambaroust SJ, Karimzadeh Halimi F, Mohammadzadeh Pakdel P, Safarzadeh H. Decontamination of methylene blue from aqueous media using alginate-bonded polyacrylamide/carbon black nanocomposite hydrogel. *Polym Adv Technol*. 2024;35(3).
15. Ren H, Gao Z, Wu D, Jiang J, Sun Y, Luo C. Efficient Pb(II) removal using sodium alginate-carboxymethyl cellulose gel beads: Preparation, characterization, and adsorption mechanism. *Carbohydr Polym*. 2016;137:402-409.
16. Ihsanullah, Abbas A, Al-Amer AM, Laoui T, Al-Marri MJ, Nasser MS, et al. Heavy metal removal from aqueous solution by advanced carbon nanotubes: Critical review of adsorption applications. *Sep Purif Technol*. 2016;157:141-161.
17. Dhiman J, Prasher SO, ElSayed E, Patel RM, Nzediegwu C, Mawof A. Heavy metal uptake by wastewater irrigated potato plants grown on contaminated soil treated with hydrogel based amendments. *Environmental Technology and Innovation*. 2020;19:100952.
18. Liu P, Yan T, Zhang J, Shi L, Zhang D. Separation and recovery of heavy metal ions and salt ions from wastewater by 3D graphene-based asymmetric electrodes via capacitive deionization. *Journal of Materials Chemistry A*. 2017;5(28):14748-14757.
19. Liang J, Yang Z, Tang L, Zeng G, Yu M, Li X, et al. Changes in heavy metal mobility and availability from contaminated wetland soil remediated with combined biochar-compost. *Chemosphere*. 2017;181:281-288.
20. Zhou Y, Tang L, Zeng G, Zhang C, Zhang Y, Xie X. Current progress in biosensors for heavy metal ions based on DNAzymes/DNA molecules functionalized nanostructures: A review. *Sensors Actuators B: Chem*. 2016;223:280-294.
21. Cheng M, Zeng G, Huang D, Lai C, Xu P, Zhang C, et al. Hydroxyl radicals based advanced oxidation processes (AOPs) for remediation of soils contaminated with organic compounds: A review. *Chem Eng J*. 2016;284:582-598.
22. Calabrese I, Cavallaro G, Lazzara G, Merli M, Sciascia L, Turco Liveri ML. Preparation and characterization of bio-organoclays using nonionic surfactant. *Adsorption*. 2015;22(2):105-116.
23. Aljeboree AM, Hussein SA, Jawad MA, Alkaim AF. Hydrothermal synthesis of eco-friendly ZnO/CNT nanocomposite and efficient removal of Brilliant Green cationic dye. *Results in Chemistry*. 2024;7:101364.
24. Acosta R, Fierro V, Martinez de Yuso A, Nabarlatz D, Celzard A. Tetracycline adsorption onto activated carbons produced by KOH activation of tyre pyrolysis char. *Chemosphere*. 2016;149:168-176.
25. Spectrophotometric Determination of phenylephrine hydrochloride drug in the existence of 4Aminoantipyrine: Statistical Study. *International Journal of Pharmaceutical Research*. 2018;10(4).
26. Taifi A, Alkadir OKA, Oda AA, Aljeboree AM, Al Bayaa AL, Alkaim AF, et al. Biosorption by Environmental, Natural and Acid-Activated Orange Peels as Low-Cost Adsorbent: Optimization of Disperse Blue 183 as a Model. *IOP Conference Series: Earth and Environmental Science*. 2022;1029(1):012009.
27. Jung H-J, Diaconescu P, Wong Y-P, Roshandel H. Facile synthesis of polyperoxides with intermolecular peroxy bonds as macroinitiators for free radical graft copolymerization. *American Chemical Society (ACS)*; 2024.
28. Aljeboree AM, Alkaim AF, Hussein SA, Abed Jawad M, Hasan I, Khuder SA. Synthesis and swelling behavior of highly adsorbent hydrogel for the removal of brilliant green from an aqueous solution: Thermodynamic, kinetic, and isotherm models. *Case Studies in Chemical and Environmental Engineering*. 2024;10:100831.
29. Bao Y, Ma J, Li N. Synthesis and swelling behaviors of sodium carboxymethyl cellulose-g-poly(AA-co-AM-co-AMPS)/MMT superabsorbent hydrogel. *Carbohydr Polym*. 2011;84(1):76-82.
30. Wang Y, Wang W, Wang A. Efficient adsorption of methylene blue on an alginate-based nanocomposite hydrogel enhanced by organo-illite/smectite clay. *Chem Eng J*. 2013;228:132-139.
31. Aljeboree AM. Removal of Vitamin B6 (Pyridoxine)

- Antibiotics Pharmaceuticals From Aqueous Systems By ZnO. *International Journal of Drug Delivery Technology*. 2019;9(02).
32. Pashaei-Fakhri S, Peighambaroust SJ, Foroutan R, Arsalani N, Ramavandi B. Crystal violet dye sorption over acrylamide/graphene oxide bonded sodium alginate nanocomposite hydrogel. *Chemosphere*. 2021;270:129419.
 33. El-Hamshary H, El-Sigeny S, Abou Taleb MF, El-Kelesh NA. Removal of phenolic compounds using (2-hydroxyethyl methacrylate/acrylamidopyridine) hydrogel prepared by gamma radiation. *Sep Purif Technol*. 2007;57(2):329-337.
 34. Shirsath SR, Patil AP, Patil R, Naik JB, Gogate PR, Sonawane SH. Removal of Brilliant Green from wastewater using conventional and ultrasonically prepared poly(acrylic acid) hydrogel loaded with kaolin clay: A comparative study. *Ultrason Sonochem*. 2013;20(3):914-923.
 35. Guilherme MR, Aouada FA, Fajardo AR, Martins AF, Paulino AT, Davi MFT, et al. Superabsorbent hydrogels based on polysaccharides for application in agriculture as soil conditioner and nutrient carrier: A review. *Eur Polym J*. 2015;72:365-385.
 36. Ghaedi M, Sadeghian B, Pebdani AA, Sahraei R, Daneshfar A, Duran C. Kinetics, thermodynamics and equilibrium evaluation of direct yellow 12 removal by adsorption onto silver nanoparticles loaded activated carbon. *Chem Eng J*. 2012;187:133-141.
 37. Shi Y, Kong X, Zhang C, Chen Y, Hua Y. Adsorption of soy isoflavones by activated carbon: Kinetics, thermodynamics and influence of soy oligosaccharides. *Chem Eng J*. 2013;215-216:113-121.
 38. Elmoubarki R, Mahjoubi FZ, Tounsadi H, Moustadraf J, Abdennouri M, Zouhri A, et al. Adsorption of textile dyes on raw and decanted Moroccan clays: Kinetics, equilibrium and thermodynamics. *Water Resources and Industry*. 2015;9:16-29.
 39. Choy KKH, Porter JF, McKay G. Langmuir Isotherm Models Applied to the Multicomponent Sorption of Acid Dyes from Effluent onto Activated Carbon. *Journal of Chemical and Engineering Data*. 2000;45(4):575-584.
 40. Mubarik S, Ehsan S, Imran M, Hanif F. Linear and nonlinear modeling of kinetics and isotherms characterizing adsorptive removal of 4-nitrophenol by biochar BC-PFP773. *Desalination and Water Treatment*. 2022;250:240-251.
 41. Patil SR, Sutar SS, Jadhav JP. Sorption of crystal violet from aqueous solution using live roots of *Eichhornia crassipes*: Kinetic, isotherm, phyto and cyto-genotoxicity studies. *Environmental Technology and Innovation*. 2020;18:100648.
 42. Sadoq M, Atlas H, Imame S, Kali A, Amar A, Loulidi I, et al. Elimination of crystal violet from aqueous solution by adsorption on naturel polysaccharide: Kinetic, isotherm, thermodynamic studies and mechanism analysis. *Arabian Journal of Chemistry*. 2024;17(1):105453.